IEEE Access
Multidisciplinary | Rapid Review | Open Access Journal

Received November 16, 2019, accepted December 6, 2019, date of publication December 13, 2019,
date of current version December 31, 2019.

Digital Object Identifier 10.1109/ACCESS.2019.2959314

Compact Four-Element MIMO Antenna System for 5G Laptops

SHU-CHUAN CHEN[1], (Member, IEEE), CHENG-WEI CHIANG[2], AND CHUNG- I G. HSU[2], (Member, IEEE)

[1]Electrical and Electronic Engineering Department, Chung Cheng Institute of Technology, National Defense University, Taoyuan 335, Taiwan
[2]Department of Electrical Engineering, National Yunlin University of Science and Technology, Yunlin 640, Taiwan

Corresponding author: Shu-Chuan Chen (scchen0319@gmail.com)

This work was supported in part by the Ministry of Science and Technology, Taiwan, under Grant MOST 107-2221-E-606-004-.

ABSTRACT This paper presents a compact dual-band four-element multiple-input multiple-output (MIMO) antenna system for the fifth-generation (5G) laptops with a large display-to-body ratio. The four antenna elements, each being a three-dimensional inverted-F antenna (IFA) of the same structure and size, are constructed on the same T-cross-sectioned substrate, the vertical part of which is embedded in the 1×64 mm^2 clearance area created from the upper edge of the display ground plane. They are configured into two dual-antenna units. Within each unit, the two IFAs are arranged to be skew-symmetric with respect to the display ground plane, and their short-circuit points are brought close to each other to achieve the so-called short-circuit decoupling. In addition, the two units are mirror imaged of each other with a small gap in between and are connected by two decoupling chip inductors to form a high-isolation four-element MIMO antenna system. In the operating bands of 3300–3600 and 4800–5000 MHz required by 5G, the measured isolation is larger than 10 dB, and the measured antenna efficiency is beyond 35 %, both being large enough for practical applications. In particular, the proposed MIMO antenna system has a profile height of only 1.4 mm, which is very small, making it suitable for laptops with a large display-to-body ratio.

INDEX TERMS Laptop antennas, multi-input multi-output (MIMO) antennas, IFA, chip inductors, self-resonant frequency.

I. INTRODUCTION

Recently, with most consumers' preference for lightweight laptops having a large display, a series of light, large-display laptops have been launched on the market. For a laptop with a fixed body, the larger the display, the narrower the bezel, and the larger the display-to-body ratio. In the pursuit of lightweight and narrow-bezel features for a laptop, the antenna mounted around the bezel of a laptop must have not only a small size but also a low profile.

In current mainstream fourth-generation (4G) mobile communication devices, in order to meet the demand for visual enjoyment of a large display, designing miniaturized low-profile antennas has been a trend [1]–[9]. Some antennas have been integrated with the ground planes and surrounding metal frames [1]–[3]. In [1], an asymmetric T-shaped slot structure with its open end aligned with the open gap of the outer side frame is excited by the low- and high-band feeds to produce the wide-enough low and high operating bands, respectively. In [2], a defected metal ground plane and an open outer side frame are integrated to form an open slot structure, which is excited by an embedded multi-strip monopole antenna to generate operating bands for long-term evolution (LTE) and wireless wide-area network (WWAN) applications. In [3], a U-shaped slot with its two open ends aligned with two open gaps of the outer side frame is divided into two inverted-L slots by a U-shaped strip to produce two wide operating bands with the aid of a low-pass and a high-pass matching circuit. In the past, antennas were frequently printed on a thin substrate and then arranged to be parallel with and above the display ground plane of a laptop [4]–[6]. These planar structures in conjunction with the complete display ground plane often cause the laptop to require a wide bezel area, which is not suitable for the current development trend of large display-to-body ratios for mobile communication devices. Besides employing

The associate editor coordinating the review of this manuscript and approving it for publication was Chow-Yen-Desmond Sim.

three-dimensional structures to achieve miniaturization and a low profile for the designed antenna, sometimes one can use chip inductors and capacitors to form matching circuits [7], [8]. Unfortunately, the cost is relatively high.

In addition to the antenna size and profile height, isolation is also an important figure of merit for a MIMO antenna system. In the design of an LTE MIMO antenna system, different isolation schemes have been explored [9]–[11]. In [9], a grounded short-strip resonator and an ungrounded folded-line resonator are employed to effectively reduce the mutual coupling between the two antenna elements in each dual-antenna unit of the four-element MIMO antenna system. However, the ungrounded resonator for decoupling purpose is coplanar with and stacked on the dual-antenna unit itself, causing the profile height of the MIMO antenna system to have an excessively large value of 18 mm. The MIMO antenna system with such a large profile height is obviously not suitable for laptops with a large display-to-body ratio. For 4G laptop applications, the MIMO antenna system if constructed on the bezel area usually requires a profile height of at least 7 mm, which sets a limit for the laptop's display-to-body ratio. To further maximize the display-to-body ratio of a laptop, the 4G MIMO antenna system can be embedded in the hinge slot [10] or constructed in the lower display ground plane that is close to the hinge slot [11]. In both cases, the hinge slot can be employed to enhance the isolation. Although clever and requiring a very small bezel area, the two-element MIMO antenna systems proposed in [10] and [11] are not easy to be extended to comprise four antenna elements, which are frequently adopted in the fifth-generation (5G) communication.

Note that it is easier for the 5G MIMO antenna system to have a low profile than for the 4G one. This is because the low-frequency limit for the former is much higher than that for the latter. Hence, it is easier for the 5G MIMO antenna system to be deployed in the bezel area near the upper display ground plane than for the 4G one if the laptop has a large display-to-body ratio. However, usually more antenna elements are needed in a 5G MIMO antenna system than in a 4G one. If in a laptop the space allowed for constructing the 5G MIMO antenna system is not large enough, the spacing between the antenna elements of the 5G MIMO antenna system will be small. Thus, how to realize a compact 5G multi-element (say, four-element) MIMO antenna system while still having good isolation poses a great challenge.

In recent years, several multi-element MIMO antenna systems with different compact configurations have been proposed for different communication devices [12]–[21]. In these studies, methods for optimizing the isolation among densely deployed antennas have also been presented. In [12]–[14], the spacing between the antenna elements in a sub-6-GHz 5G MIMO antenna system is about 15 to 30 mm, which may be considered to be large. In order to minimize the spacing between two adjacent antenna elements in a MIMO antenna system so that a satisfactory isolation can still be obtained, a chip inductor is added between the nearest ends of the two antennas [15], [16], and a capacitor-loaded shorting strip is used as the common section of two coupled-fed loop antennas so that the two antennas have no physical spacing in between [17]. In [18], the two antennas with a profile height of only 4 mm in the two-element MIMO antenna system for the 3.6-GHz LTE operation are excited with different mechanisms, so that the different near-field characteristics lead to an isolation of larger than 12 dB even without any additional decoupling component inserted in the small spacing of only 2 mm. In [19]–[21], the short-circuit decoupling technique is employed to achieve good isolation between the two antenna elements of a dual-antenna unit deployed on the 7-mm-wide side-edge frame of a smartphone. The extremely compact self-decoupling dual-antenna unit can be used as the building block for constructing massive MIMO arrays, as demonstrated in [20] and [21]. However, a large spacing between two such dual-antenna units is still required, and a compact building block comprising four closely spaced antenna elements is still in great demand for 5G wireless communications.

In this paper, we will present a new dual-band sub-6-GHz 5G four-element MIMO antenna system for laptops with a large display-to-body ratio. The four antenna elements are constructed on a T-cross-sectioned substrate that is formed by a vertical and a horizontal substrate. The vertical substrate is embedded in a clearance area that is located at the upper edge of the display ground plane and that is 45 mm away from the left edge. The four sub-6-GHz 5G antenna elements, each being a three-dimensional inverted-F antenna (IFA) of the same structure and size, are constructed on the same substrate and occupy a small space of only $1.4 \times 64 \times 3$ mm^3. The salient feature of the proposed design is that the profile height is only 1.4 mm, which is very small. The four antenna elements are divided into two dual-antenna units, in each of which the short-circuit decoupling structure can effectively enhance the isolation between the two antenna elements in the same unit. Moreover, the two dual-antenna units are deployed to be mirrored imaged of each other with a small spacing of only 1 mm. Two appropriate decoupling chip inductors are placed in the spacing to connect the two units so as to improve the isolation in between. The resulting four-element MIMO antenna system, although extremely compact, possesses good isolation, and hence can be used as the building block for constructing a massive MIMO antenna system. The fabricated sub-6-GHz 5G MIMO antenna system can cover the dual-band operation of 3300–3600 and 4800–5000 MHz. The measured isolation is over 10 dB, the envelope correlation coefficients (ECCs) calculated from the measured radiation patterns are all less than 0.3, and the measured antenna efficiency (i.e., the measured realized radiation efficiency) is larger than 35%.

II. PROPOSED MIMO ANTENNA SYSTEM DESIGN

A. MIMO ANTENNA SYSTEM STRUCTURE

Figure 1 shows the overall configuration of the proposed dual-band four-element MIMO antenna system mounted

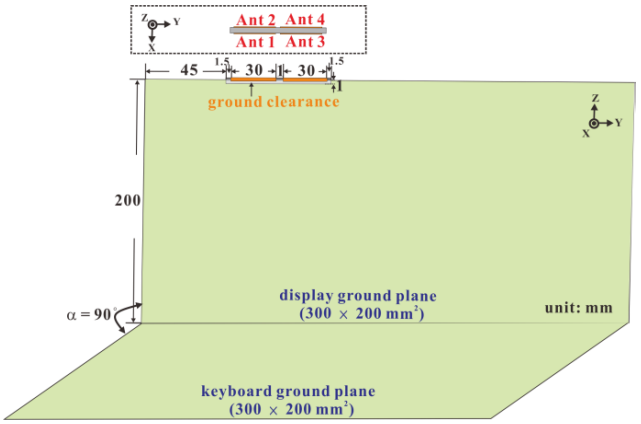

FIGURE 1. The overall structure of the proposed 5G four-element MIMO antenna system.

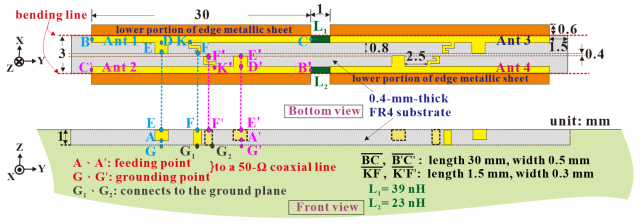

FIGURE 2. The detailed structure of the proposed 5G four-element MIMO antenna system.

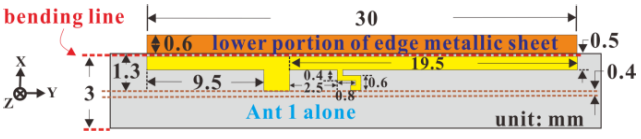

FIGURE 3. The zoom-in bottom-view plot of Ant 1 alone.

around the top edge of a laptop. The 0.2-mm-thick copper display and keyboard ground planes of the laptop have the same size of 300 × 200 mm^2, which is widely adopted in many 13-inch laptops on the market. A 1 × 64 mm^2 clearance area is created from the top edge of the display ground plane and is 45 mm away from the display ground plane's upper-left corner. The four antenna elements, designated by Ant 1, Ant 2, Ant 3, and Ant 4, are constructed on the two mutually perpendicular 0.4-mm-thick FR4 substrates of dielectric constant 4.4 and loss tangent 0.02. The 64 × 3 mm^2 horizontal substrate, which is perpendicular to the display ground plane, and the 64 × 1 mm^2 vertical substrate, which is parallel to the same ground plane, have a T-shaped cross-section. For simplicity, they will be referred to as the T-cross-sectioned substrate. Figure 2 shows the metal pattern on the bottom side of the horizontal substrate (bottom view) and the metal pattern on the vertical substrate, with a few structural dimensions given. Note that the vertical substrate is embedded in the clearance area.

Since the four antenna elements are all three-dimensional inverted-F antennas (IFAs) of the same structure and size, more detailed structural dimensions are marked in the zoom-in bottom-view plot of only Ant 1 (see figure 3). The metal

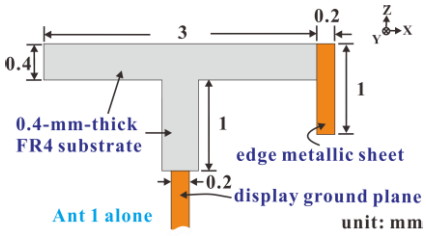

FIGURE 4. The zoom-in side-view plot of Ant 1 alone.

pattern of the IFA includes three parts: the feeding part, the main radiating part, and the short-circuit part. The feeding part comprises the $\overline{AE}$ section printed on the vertical substrate and the $\overline{DE}$ section printed on the horizontal substrate; both sections have the same width of 1 mm. The main radiating part is the 0.5 × 30 mm^2 $\overline{BC}$ section printed on the horizontal substrate in union with the 1-mm-wide, 30-mm-long, and 0.2-mm-thick edge metallic sheet that is perpendicular to the horizontal substrate. The $\overline{BC}$ section and the edge metallic sheet are soldered together along the bending line indicated in figures 2 and 3. As can be seen in the zoom-in side view given in figure 4, the top edge of the edge metallic sheet is aligned with the top substrate surface such that the edge metallic sheet below and above the bottom surface of the horizontal substrate has a width of 0.6 and 0.4 mm, respectively. The short-circuit part consists of the 0.3-mm-wide $\overline{KF}$ section printed on the horizontal substrate and the vertical 0.5-mm-wide $\overline{FG_1}$ section printed on the vertical substrate. Moreover, this IFA is connected to the center and outer conductors of the feeding mini coaxial cable through points A and G, respectively, where point G is on the display ground plane. In the proposed design, the four antenna elements are divided into two dual-antenna units, Ants 1 and 2 for the first unit and Ants 3 and 4 for the second. For more clearly perceiving the entire structure of the antenna system, the perspective views of the metal patterns of (A) Ant 1 alone, (B) Ant 2 alone, (C) the first dual-antenna unit, and (D) all four antenna elements are shown in figures 5(A), 5(B), 5(C), and 5(D), respectively. Note that the designed four-element MIMO antenna system occupies a small size of only 1.4 × 64 × 3 mm^3. The small profile height of only 1.4 mm makes the designed MIMO antenna system suitable for laptops with a large display and a narrow bezel.

As will be demonstrated later, the longer arm of the main radiating part of each IFA is associated with the lower operating frequency, and the shorter arm with the higher operating frequency. Hence, to enhance the isolation between the two antenna elements in the same dual-antenna unit, they are deployed to be skew-symmetric with respect to the display ground plane so that the longer arm of one antenna is closer to the shorter arm than to the longer arm of the other antenna, or vice versa. In addition, their shorting points (e.g., G_1 and G_2 in the first unit) are brought close to each other to achieve the so-called short-circuit decoupling [8], [9].

Next, we will discuss the isolation between the two dual-antenna units. If they are directly placed side by side, then

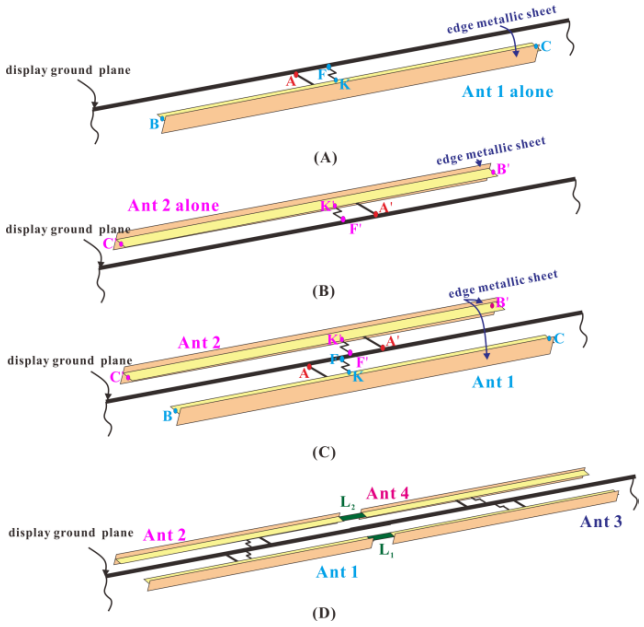

FIGURE 5. Perspective views of the metal patterns of (A) Ant 1 alone, (B) Ant 2 alone, (C) the first dual-antenna unit, and (D) all four antenna elements.

the two diagonally adjacent shorter arms belonging to the two different units will easily couple signals from one to the other, a phenomenon which also applies to the two diagonally adjacent longer arms. In such a case, the two units must be separated by a large distance to enhance the isolation in between. However, this will increase the size of the MIMO antenna system, an outcome that is undesirable. Instead of placing the two dual-antenna units side by side, we will arrange them to be mirror imaged of each other and separate them by a small gap of only 1 mm. As a result, the two shorter (longer) arms of Ants 1 and 3 (Ants 2 and 4) are on the two far ends of the substrate (see fig. 2), leading to small mutual coupling between Ants 1 and 3 (Ants 2 and 4) around the higher (lower) operating frequency. However, the two longer (shorter) arms of Ants 1 and 3 (Ants 2 and 4) on the two sides of the gap are just facing each other, causing strong mutual coupling between Ants 1 and 3 (Ants 2 and 4) around the lower (higher) operating frequency. To overcome this highly undesired drawback, we will insert a chip inductor L_1 (L_2) in the gap between the two longer (shorter) arms of Ants 1 and 3 (Ants 2 and 4) such that the chip inductor has a self-resonant frequency close to the lower (higher) operating frequency. At the self-resonant frequency, the inductor will have an infinite impedance, thus acting as a bandstop circuit and raising the isolation [21], [22]. Of course, we expect the chip inductor to have a smaller inductance value if its signal-rejecting function should occur at the higher operating frequency. The chosen inductance values are $L_1 = 39$ nH and $L_2 = 22$ nH, as indicated in Figure 2.

B. EXPERIMENT AND MEASUREMEMT RESULTS

Figure 6 shows the photo of the 5G four-element MIMO antenna system integrated with the display and keyboard

FIGURE 6. Photo of the fabricated 5G four-element MIMO antenna system integrated with the laptop.

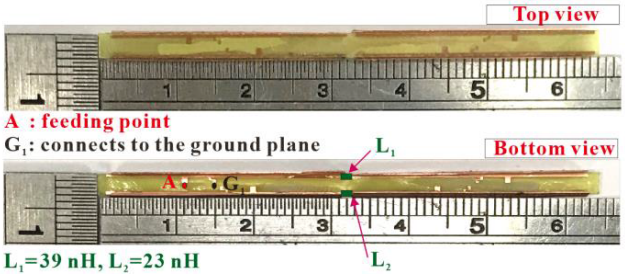

FIGURE 7. Top- and bottom-view photos of the fabricated 5G four-element MIMO antenna system.

ground planes of a laptop, and figure 7 presents the top- and bottom-view photos of the MIMO antenna system itself. The antenna was fabricated according to the dimensions given in Figures 1–4 with mm as the unit. The commercial software ANSYS HFSS (Version 15) [23] is used to carry out the simulation, with the reflection coefficient of less than –6 dB (i.e. VSWR = 3:1) as the impedance-matching criterion for the operating band. This criterion has been widely adopted for antennas implemented for mobile communication devices [12]–[21]. However, for the isolation among antenna elements in a MIMO antenna system, the transmission coefficient of less than –10 dB or even smaller has been preferably used as the criterion [10].

Figures 8 and 9 present the simulated and measured *S*-parameters of the designed 5G four-element MIMO antenna system, respectively. From the simulated and measured reflection coefficients, one can see that the designed MIMO antenna system can support the dual-band operation for the sub-6-GHz 5G wireless communication. The simulated reflection coefficients show that all the four antenna elements can generate two resonance modes, and the simulated transmission coefficients can meet the isolation requirement in the two operating bands. Although the measured results also meet the impedance-matching and isolation requirements, they slightly differ from the simulated ones. The discrepancies could be due to the fact that the additional

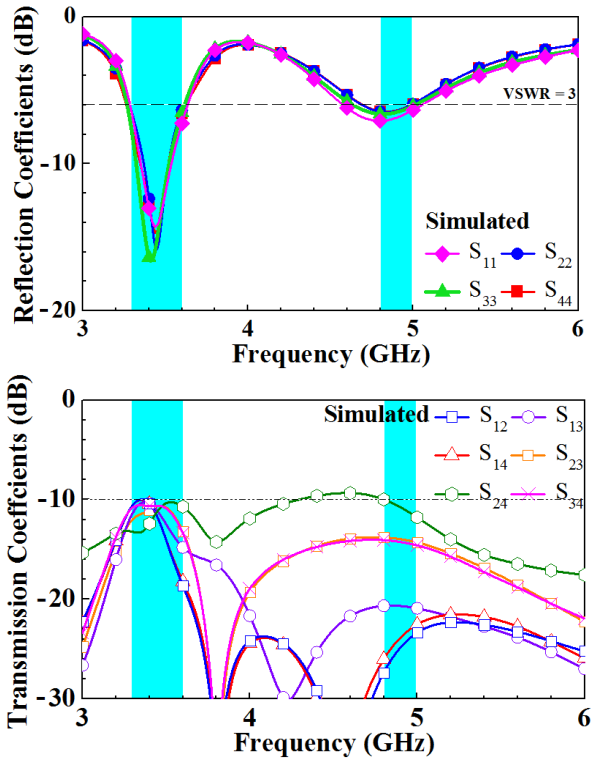

FIGURE 8. Simulated S-parameters of the proposed four 5G MIMO antennas system.

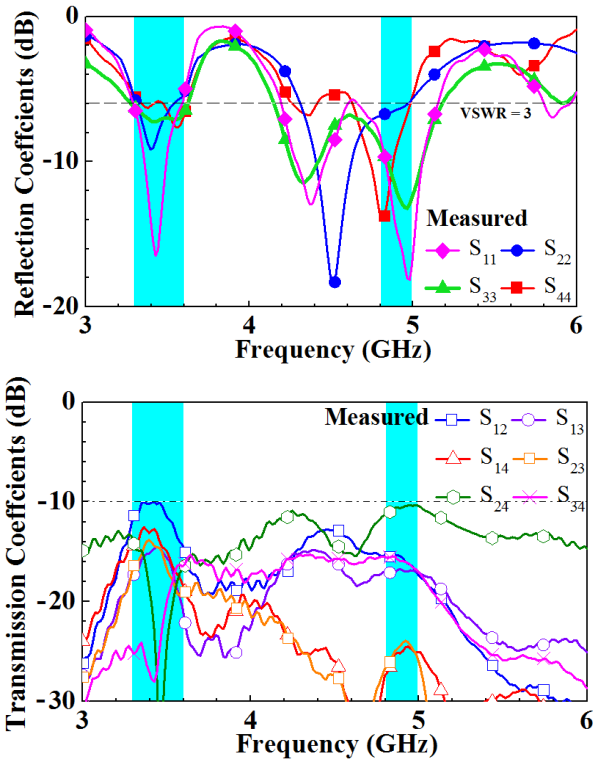

FIGURE 9. Measured S-parameters of the proposed four 5G MIMO antennas system.

mini coaxial cables used in measurement are not considered in simulation. Moreover, the parameter variation of the

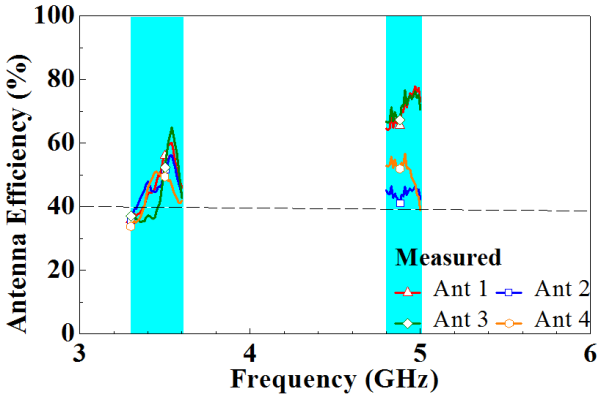

FIGURE 10. Measured antenna efficiencies for Ants 1, 2, 3, and 4.

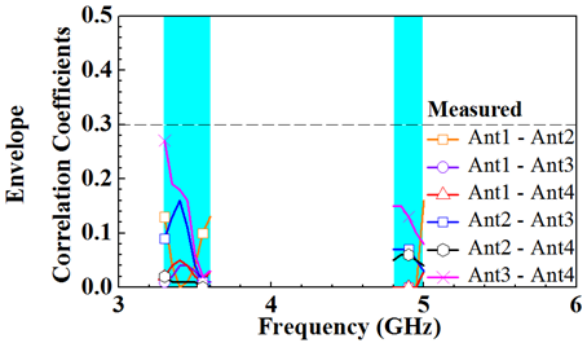

FIGURE 11. Calculated ECCs from measured radiation patterns of the 5G four-element MIMO antenna system.

FR4 substrate and the imperfection in fabrication could also be part of the reasons for the discrepancies.

Figure 10 shows the simulated and measured antenna efficiencies when only one of the antenna elements of the MIMO antenna system is excited and the other three are silent (i.e., the other three antenna elements are terminated by a 50-Ω load). The measured antenna efficiencies in the operating bands are in the range of 35% to 80%, which are large enough for practical applications for such a compact MIMO antenna system. Note that these efficiencies are measured and simulated in the presence of the display and keyboard ground planes. Hence, besides the currents excited on the four antenna elements, the currents induced on the ground planes also contribute to the efficiencies although these ground-plane currents are relatively small as can be seen from current-distribution plots illustrated later in this paper.

In addition to the isolation between antenna elements in the MIMO antenna system, the ECC is also an important performance parameter of the MIMO antenna system [24]. Generally speaking, the ECC of less than 0.5 is the criterion for practical applications [25]. Figure 11 shows the ECCs calculated from the measured radiation patterns of the four antenna elements. These ECCs are all less than 0.3 in the two operating bands, proving that the four antenna elements have good channel independence under such a configuration.

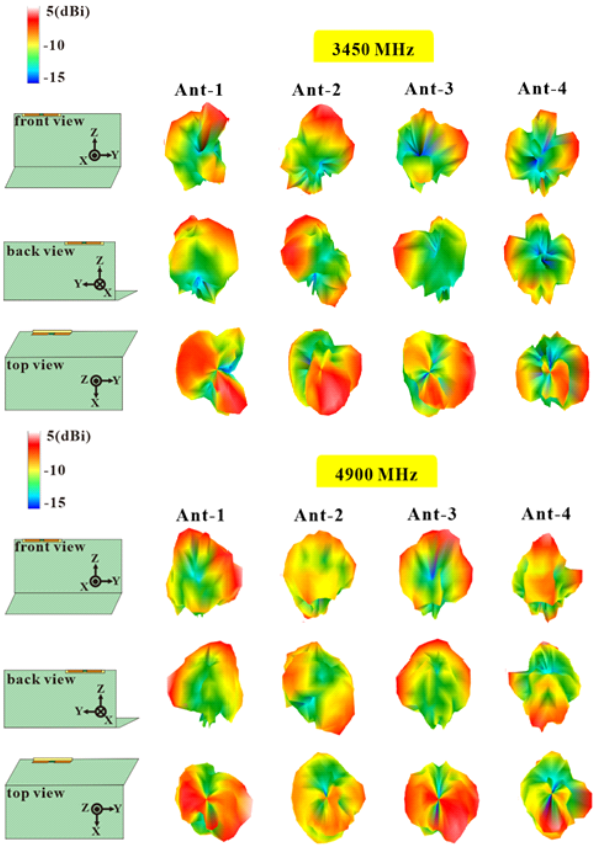

FIGURE 12. Measured 3D radiation patterns of the four antenna elements at 3450 and 4900 MHz.

Figure 12 shows at 3450 and 4900 MHz the 3D radiation patterns when only one of the four antenna elements is excited. The patterns are viewed from the $+x$, $-x$, and $+z$ directions. As can be seen from the figure, the far-field radiation patterns of the four antennas are quite different. This is why the ECCs in the operating frequency bands shown in figure 11 are less than 0.3. Thus, the far-field radiation patterns of the four antenna elements are independent and suitable for the MIMO operation.

The proposed MIMO antenna system is also compared with other published relevant MIMO antenna systems in terms the size of the 2-antenna array (i.e., the size of the dual-antenna unit), operating bands, spacing between the two antennas in a 2-antenna array, spacing between two 2-antenna arrays, isolation, and efficiency, as presented in Table 1. Note that all the MIMO antenna systems in this table are constructed on some FR4 printed-circuit boards (PCBs). The PCBs of [13], [14], [18], and [19] are arranged parallel to the system ground planes, whereas those of [20], [21] and this work are perpendicular to the ground planes. For all the latter three antennas, a 1-mm-wide clearance area is created in the ground planes. Hence, for size comparison in the second column of Table 1, we will show only the width and length of the PCB used in each of the antenna systems. In all these antenna systems, two antenna elements can be grouped as a 2-antenna array. Clearly, our proposed

TABLE 1. Comparison of the presented design with the recently reported 5G terminal MIMO antennas.

Ref.	2-antenna array size (width × length) (mm)	operating bands (MHz)	spacing between two antennas (mm)	spacing between 2-antenna arrays (mm)	Isolation (dB)	efficiency
13	3 × 31	3400~3800	15	15	≥ 10	≥ 42%
14	3 × 57.8	3400~3800 5150~5925	≥ 19.5	≥ 19.5	≥ 10	≥ 42%
18	4 × 30	3400~3800	without spacing	unanalyzed	≥ 12	≥ 57%
19	4 × 30	3400~3800	without spacing	unanalyzed	≥ 14	≥ 57%
20	7 × 15	3400~3600 5725~5875	without spacing	20	≥ 15	≥ 55%
21	4.2 × 35	3300~3600	3 mm	unanalyzed	≥ 12	≥ 56%
this work	3 × 30	3300~3600 4800~5000	without spacing	1	≥ 10	≥ 35%

2-antenna array occupies the smallest area. If two 2-antenna arrays are to be formed a 4-antenna building block, the spacing between the two 2-antenna arrays should be considered. As shown in this table, our proposed MIMO antenna system has the smallest spacing of only 1 mm between two 2-antenna arrays while maintaining good isolation and antenna efficiencies, and hence can be used as a building block for constructing a MIMO antenna system with more elements. Although the isolation of the MIMO antenna system in [20] is larger than 15 dB, its large spacing between two 2-antenna arrays might be considered as a disadvantage in the construction of a massive MIMO antenna system. Although Reference [18]–[21] all show an efficiency of larger than 50% for their MIMO antenna systems, they have not considered forming a 4-element MIMO antenna system except for [21]. In short, our proposed MIMO antenna system consisting of four elements is compact enough to be easily arranged on the top edge of a screen with a border thickness of only 3 mm to cover 3400–3600 and 4800–5000 MHz.

C. MIMO ANTENNA SYSTEM CHARACTERISTICS ANALYSIS

To further explore the isolation between the two antenna elements of the dual-antenna unit and to prove that the two closely spaced short-circuit metal parts of the dual-antenna unit form an effective decoupling structure, we also analyze the current distributions around the two antenna elements in the first dual-antenna unit. Figure 13 shows the current distributions of the dual-antenna unit operating at 3450 and 4900 MHz. At both frequencies, strong ground-plane currents when only Ant 1 (2) is excited is directed to the short-circuit metal part of Ant 2 (1) without directly entering the port of Ant 2 (1). Therefore, no significant signal is coupled from one antenna element to the other, leading to satisfactory isolation in between.

Next, we will study the mutual coupling between the two dual-antenna units by examining the electric currents on the MIMO antenna system itself and the surrounding portion of

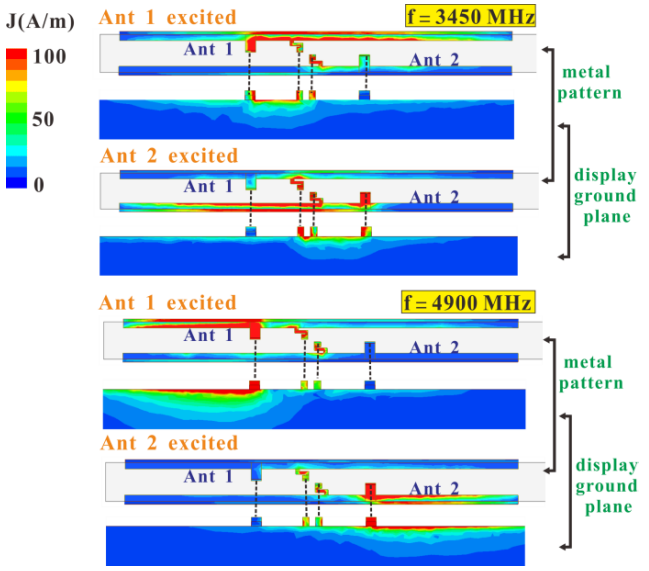

FIGURE 13. Current distributions of the first dual-antenna unit at 3450 and 4900 MHz.

the display ground plane. To make the MIMO antenna system compact, we have arranged the two dual-antenna units to be mirror imaged of each other with a small gap of only 1 mm in between. To avoid the resulting strong coupling between Ants 1 and 3 (Ants 2 and 4) at 3450 (4900) MHz, respectively, two decoupling chip inductors have been inserted between the two dual-antenna units. The electric current distributions for the MIMO antenna system with and without the chip inductors will be compared. Two scenarios have been considered: the case where Ant 1 or 3 is excited at 3450 MHz and the case where Ant 2 or 4 is excited at 4900 MHz. Figures 14 and 15 present the electric current distributions with and without the decoupling chip inductors, respectively, at both operating center frequencies. In all the cases considered, no significant display ground plane currents are induced around the silent dual-antenna unit if with the decoupling chip inductors. On the contrary, if without the chip inductors, the currents around the silent dual-antenna unit are much stronger. These results signify that the chip inductors do play a very important role of decoupling the two dual-antenna units. Note that, whether with or without the chip inductors, the electric currents appearing on the ports of the silent antennas for the case where Ant 1 or 3 is excited at 4900 MHz and for the case where Ant 2 or 4 is excited at 3450 MHz are also relatively small and hence are not shown here for brevity. This is because in these cases the shorter (longer) arm excited at 4900 (3450) MHz in Ant 1 (2) is far away from the shorter (longer) arm in Ant 3 (4).

Figure 16 shows the comparison between the transmission coefficients with and without the chip inductors. It can be seen from the figure that adding two chip inductors between the two dual-antenna units can enhance the isolation by 1 to 4 dB in the low-frequency band and by about 7 dB in the high-frequency band.

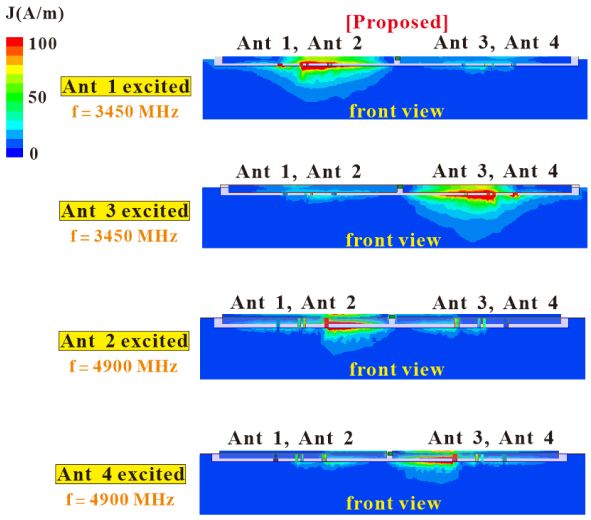

FIGURE 14. Current distributions around the four antenna elements at 3450 and 4900 MHz with chip inductors.

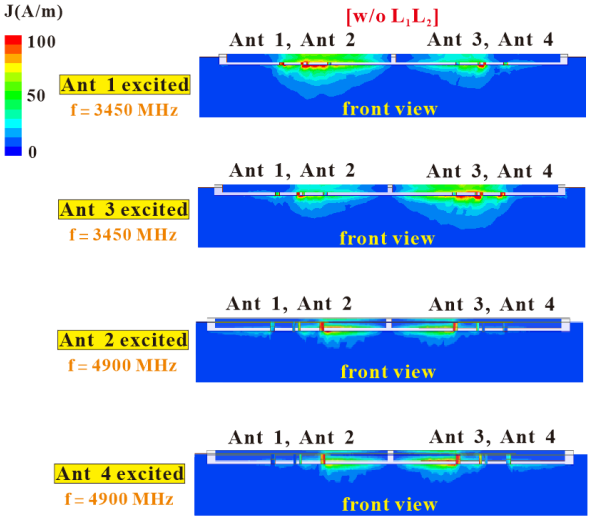

FIGURE 15. Current distributions around the four antenna elements at 3450 and 4900 MHz without chip inductors.

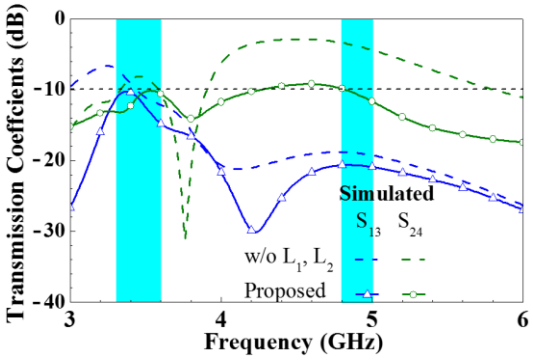

FIGURE 16. Comparison between the transmission coefficients with and without chip inductors.

D. PARAMETRIC STUDIES

To further understand the operating mechanism of the designed IFA itself, we compare in figure 17 simulated

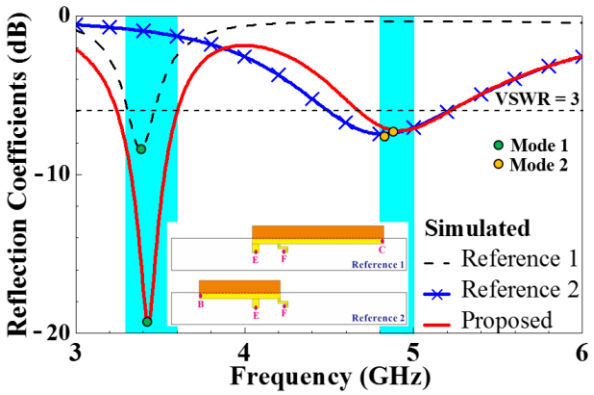

FIGURE 17. Simulated reflection coefficients of the Reference 1, Reference 2, and proposed IFAs.

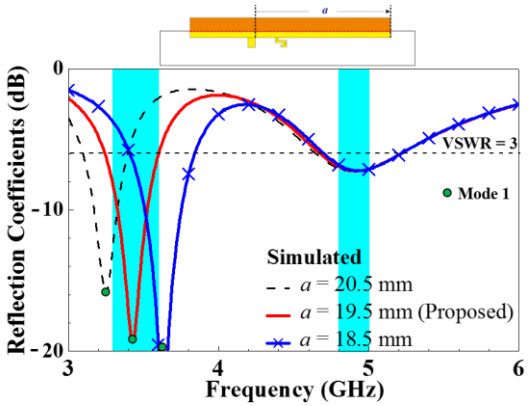

FIGURE 18. Simulated reflection coefficients of the dual-band IFA for three different values of *a*.

reflection coefficients of three different IFA structures. They include the proposed one, the one with the longer arm only (Reference 1), and the one with the shorter arm only (Reference 2). The last two of the three IFA structures are given in the inset of figure 17 for easy reference. Clearly, the Reference 1 IFA produces only the resonance mode (called Mode 1) around 3450 MHz. The Mode 1 current is distributed from the feeding point to the open end of the longer arm, which for brevity is not shown here. Similarly, the Reference 2 IFA generates a resonance mode (named Mode 2) around 4900 MHz, whose corresponding current distribution is from the feeding point to the open end of the shorter arm. When these two structures are combined to form the proposed dual-band IFA, the resulting operating frequencies are wide enough to cover 3300–3600 and 4800–5000 MHz required by 5G.

From the results given in figure 17, we expect that the length of the longer (shorter) arm, denoted by a (b), can be varied to independently fine tune the low-frequency (high-frequency) band. This expectation is validated in figures 18 and 19. In figure 18, the longer arm (with length a) of the dual-band IFA is shortened from 20.5 to 18.5 mm, causing the dip frequency of the low-frequency band to increase from 3.25 to 3.62 GHz. By contrast, the reflection-coefficient

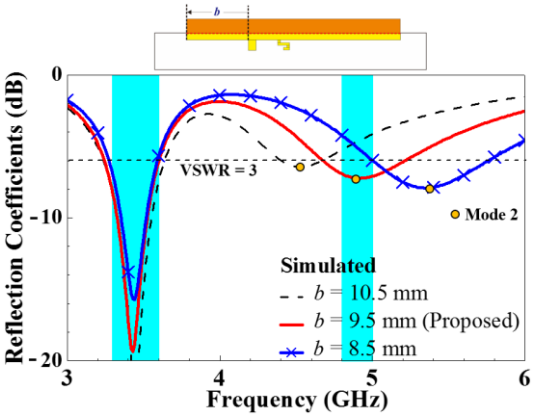

FIGURE 19. Simulated reflection coefficients of the dual-band IFA for three different values of *b*.

curves around the high-frequency band remain almost the same. In figure 19, the shorter arm (with length b) of the dual-band IFA is shortened from 10.5 to 8.5 mm, leading to the increased dip frequency for the high-frequency band. By contrast, the reflection-coefficient curves around the low-frequency band are only slightly affected. In short, the longer (shorter) arm is associated with the low-frequency (high-frequency) band.

III. CONCLUSION

In this paper, a novel four-element MIMO antenna system has been designed for 5G laptop applications. The MIMO antenna system is compact, measuring only 1.4 × 64 × 3 mm^3. The profile of the antenna system has a height of only 1.4 mm, which is a small value among 3D MIMO antenna systems, making it suitable for laptops with a large display-to-body ratio and a narrow bezel. The antenna elements in the proposed MIMO antenna system are structurally simple, and their two operating bands can each be independently adjusted by varying only one structural parameter. The measured operating bands of the MIMO antenna system are wide enough to cover 3300–3600 and 4800–5000 MHz required by sub-6-GHz 5G. In these two 5G bands, the ECCs calculated from the measured radiation patterns are less than 0.3, and the measured antenna efficiencies are larger than 35%. In addition, although densely deployed, the four antenna elements are cleverly configured so that all in-band isolations are larger than 10 dB.

REFERENCES

[1] K.-L. Wong and C.-Y. Tsai, "Low-profile dual-wideband inverted-T open slot antenna for the LTE/WWAN tablet computer with a metallic frame," *IEEE Trans. Antennas Propag.*, vol. 63, no. 7, pp. 2879–2886, Jul. 2015.

[2] S.-C. Chen, C.-C. Huang, and W.-S. Cai, "Integration of a low-profile, long-term evolution/wireless wide area network monopole antenna into the metal frame of tablet computers," *IEEE Trans. Antennas Propag.*, vol. 65, no. 7, pp. 3726–3731, Jul. 2017.

[3] K. L. Wong and C. Y. Tsai, "Dual-wideband U-shape open-slot antenna for the LTE metal-framed tablet computer," *Microw. Opt. Technol. Lett.*, vol. 57, no. 11, pp. 2677–2683, Nov. 2015.

[4] S. C. Chen and J. Y. Sze, "Isolation-improved LTE MIMO antenna for laptop computer applications," in *Proc. ISAP*, Kaohsiung, Taiwan, Dec. 2014, pp. 425–426.
[5] J. Y. Sze, S. C. Chen, and Y. C. Chu, "Small-size LTE/WWAN coupled-fed loop antenna with distributed parallel resonant circuit," in *Proc. ISAP*, Kaohsiung, Taiwan, Dec. 2014, pp. 497–498.
[6] J.-H. Lu and Y.-M. Yan, "Planar LTE/WWAN monopole antenna for 4G tablet computer," in *Proc. IEEE Int. Symp. Antennas Propag. USNC/URSI Nat. Radio Sci. Meeting*, Vancouver, Canada, Jul. 2015, pp. 1142–1143.
[7] K. L. Wong and M. T. Chen, "Very-low-profile dual-wideband loop antenna for LTE tablet computer," *Microw. Opt. Technol. Lett.*, vol. 57, no. 1, pp. 141–146, Jan. 2015.
[8] K. L. Wong and Z. G. Liao, "Passive reconfigurable triple-wideband antenna for LTE tablet computer," *IEEE Trans. Antennas Propag.*, vol. 63, no. 3, pp. 901–908, Mar. 2015.
[9] W. Y. Li, W. J. Chen, and C. Y. Wu, "Multiband 4-Port MIMO antenna system for LTE700/2300/2500 operation in the laptop computer," in *Proc. APMC*, Kaohsiung, Taiwan. Dec. 2012, pp. 1163–1165.
[10] S. C. Chen and C. S. Fu, "Switchable long-term evolution/wireless wide area network/wireless local area network multiple-input and multiple-output antenna system for laptop computers," *IEEE Access*, vol. 5, pp. 9857–9865, 2017.
[11] S. C. Chen, P. W. Wu, C.-I. G. Hsu, and J. Y. Sze, "Integrated MIMO slot antenna on laptop computer for eight-band LTE/WWAN operation," *IEEE Trans. Antennas Propag.*, vol. 66, no. 1, pp. 105–114, Jan. 2018.
[12] Y.-L. Ban, C. Li, C.-Y.-D. Sim, G. Wu, and K.-L. Wong, "4G/5G multiple antennas for future multi-mode smartphone applications," *IEEE Access*, vol. 4, pp. 2981–2988, 2016.
[13] K. L. Wong and J. Y. Lu, "3.6-GHz 10-antenna array for MIMO operation in the smartphone," *Microw. Opt. Technol. Lett.*, vol. 5, pp. 1699–1704, Jul. 2015.
[14] Y. Li, C.-Y.-D. Sim, Y. Luo, and G. Yang, "Multiband 10-antenna array for sub-6 GHz MIMO applications in 5-G smartphones," *IEEE Access*, vol. 6, pp. 28041–28053, 2018.
[15] K. L. Wong and L. Y. Chen, "Dual inverted-F antenna with a decoupling chip inductor for the 3.6-GHz LTE operation in the tablet computer," *Microw. Opt. Technol. Lett.*, vol. 57, pp. 2189–2194, Sep. 2015.
[16] S.-W. Su, C.-T. Lee, and S.-C. Chen, "Very-low-profile, triband, two-antenna system for WLAN notebook computers," *IEEE Antennas Wireless Propag. Lett.*, vol. 17, no. 9, pp. 1626–1629, Sep. 2018.
[17] K. L. Wong, B. W. Lin, and S. E. Lin, "High-isolation conjoined loop MIMO antennas for the 5G tablet devices," *Microw. Opt. Technol. Lett.*, vol. 61, pp. 111–119, Jan. 2019.
[18] K.-L. Wong and H.-J. Chang, "Hybrid dual-antenna for the 3.6-GHz LTE operation in the tablet computer," *Microw. Opt. Technol. Lett.*, vol. 57, pp. 2592–2598, Nov. 2015.
[19] K.-L. Wong, C.-Y. Tsai, and J.-Y. Lu, "Two asymmetrically mirrored gap-coupled loop antennas as a compact building block for eight-antenna MIMO array in the future smartphone," *IEEE Trans. Antennas Propag.*, vol. 65, no. 4, pp. 1765–1778, Apr. 2017.
[20] K.-L. Wong, B.-W. Lin, and B. W.-Y. Li, "Dual-band dual inverted-F/loop antennas as a compact decoupled building block for forming eight 3.5/5.8-GHz MIMO antennas in the future smartphone," *Microw. Opt. Technol. Lett.*, vol. 59, no. 11, pp. 2715–2721, Nov. 2017.
[21] K. L. Wong, Y. H. Chen, and W. Y. Li, "Decoupled compact ultra-wideband MIMO antennas covering 3.3-6.0 GHz for the fifth-generation mobile and 5GHz-WLAN operations in the future smartphone," *Microw. Opt. Technol. Lett.*, vol. 60, pp. 2345–2351, Oct. 2018.
[22] I. Bahl, *Lumped Elements for RF and Microwave Circuits*. Norwood, MA, USA: Artech House, 2003.
[23] *Corporation HFSS*. Accessed: Apr. 16, 2019. [Online]. Available: http://www.ansys.com/products/electronics/ansys-hfss
[24] Y. A. S. Dama, R. A. Abd-Alhameed, S. M. R. Jones, D. Zhou, N. J. McEwan, M. B. Child, and P. S. Excell, "An envelope correlation formula for (N, N) MIMO antenna arrays using input scattering parameters, and including power losses," *Int. J. Antennas Propag.*, vol. 2011, Aug. 2011, Art. no. 421691.
[25] R. Vaughan and J. Andersen, "Antenna diversity in mobile communications," *IEEE Trans. Veh. Technol.*, vol. VT-36, no. 4, pp. 149–172, Nov. 1987.